

# Effectiveness of Belleville Washers for Seismic Retrofit of Substation Equipment

Author One<sup>1\*</sup>

Author Two<sup>2</sup>

Author Three<sup>1</sup>

January 19, 2026

## Abstract

Seattle City Light (SCL), a power utility in the Pacific Northwest where there is potential for large earthquakes, has retrofitted several Capacitive Voltage Transformers (CVT) in their substations with Belleville washer arrangements at the bases to improve seismic performance. The strategy is simple and relatively low-cost to implement, and preliminary testing at SCL has demonstrated improved seismic performance. The washer arrangements essentially function as seismic isolators, reducing the frequency and increasing damping. To expand the implementation of this strategy more broadly for other equipment and at other utilities' substations, this project systematically characterizes the stiffness and damping mechanisms of Belleville washer arrangements and tests a retrofitted 230kV CVT on an earthquake simulator. Special instrumentation is developed to monitor the mechanics of the Belleville washer arrangements including force, deformation and equipment base moment measurements. A detailed modeling and analysis procedure is developed, allowing for either a nonlinear dynamic approach or an equivalent linear dynamic approach, to predict the response of equipment such as CVTs outfitted with Belleville washer stacks for seismic protection. The analysis procedure has been validated with experimental measurements. Essentially, knowing the force-deformation response of a washer configuration, obtained for example by cyclic loading in a material testing machine, together with the inertia characteristics of the equipment, the seismic response of the equipment can be predicted. This will enable washer configurations to be designed and deployed readily for seismic protection of various equipment.

**Keywords:** Substation equipment, seismic performance improvement, nonlinear and linear dynamic analysis, Belleville washers (disc springs), damping, experimental validation

## 1 Introduction

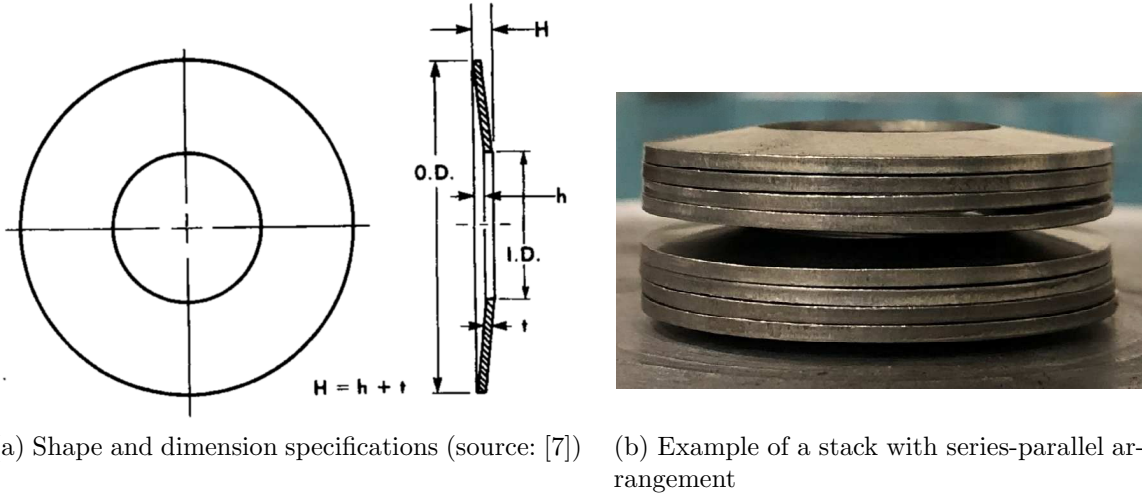
### 1.1 Background and objectives

Base isolation and supplemental damping systems are now widely used as seismic protective systems in structures. They represent a design philosophy that seeks to reduce seismic demand on functional structural components, and to minimize if not eliminate damage and permanent deformation even under large earthquakes. This is in contrast to the conventional seismic design philosophy, wherein structural components are designed to be ductile, and undergo permanent deformation without failure. For critical structures and equipment, such as in electrical substations, the approach of reducing seismic demand and permanent deformations is more attractive to ensure continued functioning of such structures and equipment post-earthquake. The concept of frequency modification for substation equipment was recommended as early as 1973 in a report prepared for Bonneville Power Administration (BPA) [1]. Base isolation and supplemental damping systems are being increasingly deployed in substations for seismic protection [2–5].

One approach to modifying frequency and adding damping is using stacks of Belleville washers. Belleville washers, named after Julian Belleville, who patented them in 1867, are circular washers given a taper to form a conical shape (Figure 1a). They are also known as a disc springs or conical spring washers, although

---

\* Author One was partially supported by Grant XXX



(a) Shape and dimension specifications (source: [7])

(b) Example of a stack with series-parallel arrangement

Figure 1: Belleville washer shape, dimensions and stack consisting of series-parallel arrangement

the term “disc springs” may be more appropriate [6] for the type of dynamic application considered in this report. When a compressive load is applied along the axis, the washer flattens by way of elastic deformation, resulting in spring action [7]. When washers are nested such that the bottom surface of one is placed on the top surface of the next, frictional rubbing between these surfaces results in hysteretic behavior (see section 3), and hence energy dissipation. The washers can also be stacked in different ways as illustrated in Figures 1 and 3. Thus the stiffness and dissipation of a stack of Belleville washers can be tuned. Testing discussed further in section 3 has shown that the force-displacement hysteresis of washer stacks is stable and repeatable. These stacks therefore lend themselves to modeling, and use as engineered frequency modification and energy dissipation devices. For early analyses of the mechanical behavior of Belleville washers, see [8,9], considering both single washer and nesting. For a more recent study on the analysis of washer mechanical behavior, see [10] and the references therein. The force-displacement behavior of a single washer is given by [7,9]

$$F = \frac{E\delta}{(1 - \mu^2)Ma^2} \left[ (h - \delta) \left( h - \frac{\delta}{2} \right) t + t^3 \right] \quad (1)$$

where  $F$  and  $\delta$  are the force in the washer and deflection,  $E$  and  $\mu$  are the Young’s modulus and Poisson ratio of the washer material,  $M$  is a constant that depends on the ratio of outer to inner diameters (see [7] for a chart),  $a$  is the outer radius and  $h$  and  $t$  are the dimension shown in Figure 1. Depending on the  $h/t$  ratio, equation (1) implies a wide variety force-displacement behaviors as shown in Figure 2. As a point of reference, the washers used in the present project are listed in Table 1-1. The K1875-G-086 washer has a  $h/t$  ratio of 0.5, which corresponds to almost linear behavior till flattening. The K1750-J-057 washer on the other hand has a  $h/t$  ratio of 1.0 resulting in a force-displacement curve that softens significantly before flattening. These behaviors are reflected in the test results in section 3. Specific features of the force-displacement behavior can be exploited<sup>1</sup>. An even wider range of behavior has been explored using Belleville washers made of shape-memory materials [12].

Belleville washers have been used in a number of industries for vibration isolation/absorption applications (see for example [13]). This includes seismic protective systems. Use of large Belleville washers (referred to therein as coned disc springs) for vertically isolation of the reactor vessel and other components in a horizontally isolated nuclear power plant building was discussed in references [14–16]. Belleville washers have been used to maintain bolt tension in frictional sliding structural connections [17]. Shape memory

<sup>1</sup>for example, by preloading washers of  $h/t$  of about 1.5 have nearly zero stiffness at flattening; so by preloading such washers to flattening and providing spacing to deformed beyond flattening, an isolation system with nearly zero frequency can be achieved (see for example [11]). Such approaches are not pursued in the present project but offer possibilities to consider in the future.

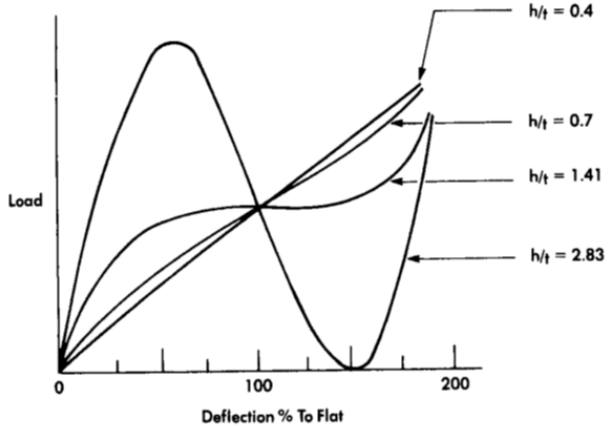


Figure 2: Force-displacement response of a single washer as a function of  $h/t$  (source [7])

Belleville washers have also been considered for energy-dissipating braces in structures [18]. The closely related concept of ring springs has been studied for seismic isolation in [19]. Use of Belleville washers for vertical isolation of buildings under train-induced vibration has been studied in [20]; in this paper, the different force-displacement responses of Figure 2 are properly utilized and a thorough analysis of hysteretic behavior (cf. section 3 in this report) is presented.

The first suggestion of using Belleville washers for seismic protection of substation equipment was in a report prepared for Bonneville Power Administration [1]. The suggestion was made in the context of lightning arresters. The 1984 edition of IEEE 693 [21] briefly mentions the possibility of Belleville washers for seismic protection, but this was removed in subsequent edition. Seattle City Light has been installing Belleville washer stacks for seismic protection of their equipment; the present research was driven by this.

The goal of this project is to study the effectiveness of Belleville washers for seismic protection of equipment such as capacitive voltage transformers (CVT), capacitor banks etc. that do not have moving parts (such as in switches) and do not have complex dynamic modes of their own (such as dead tank circuit breakers). Such equipment, when mounted on support structures, essentially behave as rigid bodies rocking under horizontal ground motion due to the flexibility of the support structure. When Belleville washer stacks are installed at the base of such equipment, above the support structure, the equipment will rock under horizontal ground motion relative to the support structure. The Belleville washer stacks are expected to provide damping through frictional dissipation under such motion, resulting in reduction of equipment base moment relative when they are rigidly connected to the support structure. In deforming to provide frictional dissipation, the washer stacks will also invariably reduce the frequency; this reduction may further aid in reducing base moment. This could potentially occur at the expense of increased terminal deflection that must be accommodated.

The objectives of this project are:

1. Develop an analysis-based systematic approach for design of a Belleville washer seismic protective system for a given equipment (together with given seismic demand and support structure).
2. Develop support for such an approach through physical experiments.

A CVT provided by Seattle City Light (see 4) is used in the shake table experiments described in section 4.

## 1.2 Nomenclature for washer configurations

The specific washers used in the project are from Key Bellevilles [22] and are listed in Table 1.

Table 1: Washers used in this project [22]

Washer	Outer diameter (in)	Inner diameter (in)	$t$ (in)	$h$ (in)	Flattening load (lb)
K1875-G-086	1.875	0.656	0.086	0.043	1319
K1750-J-057	1.750	0.88	0.057	0.057	650

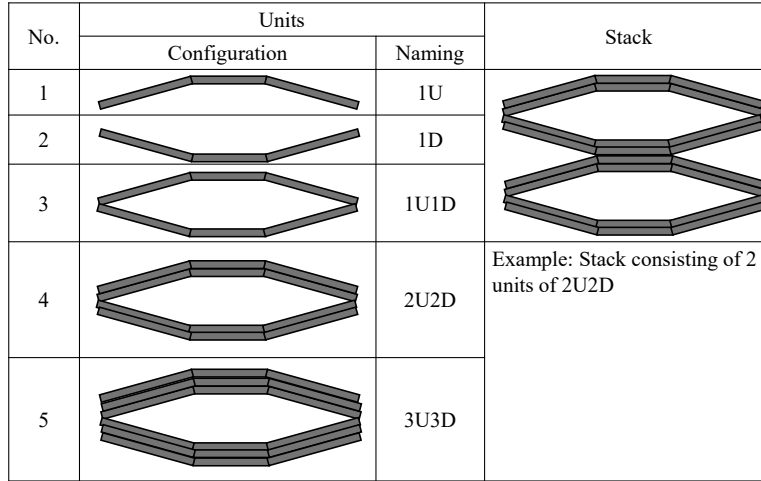


Figure 3: Nomenclature used for Belleville washer units and stacks

Figure 3 summarizes the nomenclature used in this report for Belleville washer units, each consisting of series parallel arrangements. A stack is identified by the number and type of units, for example as illustrated in Figure 3.

Then washers are nested with the cones oriented in the same direction, as for example in the top or bottom half of a 2U2D unit, they act in *parallel* since when a load is applied, their deformations are the same. When the cone orientations are opposite, as for example with the two washers in a 1U1D unit, they are in series, since they see the same force and their deformations are additive. Thus, a stack can be viewed as a series-parallel arrangement of washers. If the washers were ideal springs, the stiffness of a stack can be calculated using series-parallel combinations of the stiffnesses of the constituent springs (as will be seen in section 3), washers, particularly when nested are not linear springs and exhibit hysteresis, so such a calculation of stiffness would only be approximate). The strength (flattening load) of a stack is determined by the weakest parallel combination in the stack.

### 1.3 Analysis and design questions

The findings reported here must ultimately guide the selection of washer stacks to provide the desired level of seismic protection. This is the design question, given (a) an equipment, (b) its support structure, (c) seismic input (design spectrum) and (d) performance specifications (max base moment, max terminal displacement etc.), design a Belleville washer stack so that the system response meets the specifications.

A prerequisite to approaching this design question is being able to answer the analysis question, given (a) an equipment, (b), its support structure, (c) seismic input (ground motion record) and (d) a specific Belleville washer configuration, compute the response of this system (accelerations, base moments, terminal displacements etc.). Hence the emphasis of this project is more on this analysis question and support for the analysis process from physical experimental measurements, with a focus as noted above on “rigid” structures, in particular a CVT.

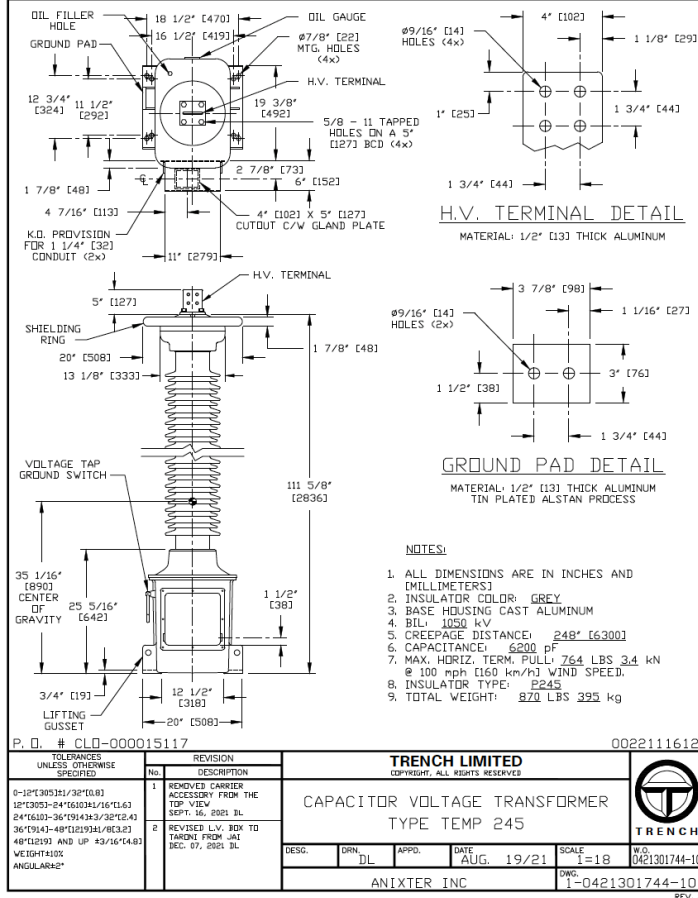


Figure 4: Capacitive voltage transformer (CVT) provided by Seattle City Light and used in shake table experiments described in section 4.

## 1.4 Organization of the report

This report is organized as follows. As noted above, the main goal of this project is to develop an analysis-based systematic approach for design of a Belleville washer seismic protective system. The report is therefore structured around an analysis procedure. This procedure is summarized upfront in section 2, and the various steps in this procedure are expounded in subsequent chapters. Characterizing the force-displacement hysteresis of a single stack of washers through cyclic loading tests is presented in section 3. Shake table experiments to characterize dynamic seismic response of a CVT equipment with Belleville washer stacks, including setup, instrumentation and specific steps for installing the washer stacks, are described in section 4. In section 5, a nonlinear dynamic model of the CVT with Belleville washer stacks is developed, and predictions from the model are compared with measurements from shake table experiments. An important note is that all the information needed for this model can be obtained from the washer characterization data from section 3, the type of information that can be readily obtained. In section 6, a linearized model based on equivalent stiffness and damping is developed that may be more conducive for practical use than the nonlinear model in section 5; this linear model can also be developed simply for the characterization data in section 3. The approach taken in this report to analyze substation equipment with Belleville washer seismic protective systems loosely parallels that in ASCE 7 for seismically isolated structures; this is pointed out in section 6 to lend credence to the proposed approach relative to well-established procedures in seismic standards. Finally in section 7, a summary is provided, and some outstanding questions are identified.

## 2 Proposed analysis procedure

The main goal of this project is to develop an analysis-based systematic approach for design of a Belleville washer seismic protective system. Therefore, in this chapter, a proposed analysis procedure is laid out. This serves to tie together the different steps and experimental support for these steps discussed in subsequent chapters. The following is the proposed analysis procedure:

Given (a) an equipment, (b) its support structure, (c) seismic input (ground motion record), (d) Belleville washer configuration

1. Determine the force-displacement response of the stack.
  - In this project, we have done this by testing the stack in a material test machine (see section 3).
  - This is a hysteretic behavior.
2. Compute the moment-rotation behavior of the assembly of washer stacks (see section 5).
  - This can be done, for example, in an Excel spreadsheet.
  - In this project, special instrumentation has been used to experimentally verify the relationship between the stack force-displacement behavior and the system moment-rotation behavior (see section 4).
3. Model this moment-rotation behavior – two possible approaches.
  - Fit a hysteresis model (section 5).
  - Compute an “equivalent” stiffness and damping (section 6).
  - Both approaches have been verified in this project; it has also been verified that this equivalent stiffness and damping agrees well with fitting a linear model to the measured response.
4. Compute the system response – three approaches are possible.
  - Nonlinear time-history analysis with the hysteresis model for the washer arrangement (section 5).
  - Linear time history analysis with the equivalent stiffness and damping.
  - Response spectrum analysis with the equivalent stiffness and damping ((section 6). This together with the equivalent stiffness and damping resemble ASCE 7 process for base isolation (Chapter -))
  - In the project, it has been verified that the three approaches produce close responses.

## 3 Cyclic force-displacement behavior of washer stacks

This chapter is on the measurement of force-displacement behavior of Belleville washer stacks. As will be seen in sections 5 and 6, this is the primary information required to predict the seismic response of rigid equipment (besides mass, moment of inertia of the equipment itself and support structure stiffness).

The force displacement response of a washer stack is obtained here by applying cyclic compressive loading to the stack in a materials testing machine. At first, this was done by simply compressing the stack between loading plates as shown in Figure 5a. The resulting force-displacement curves of Figure 5b showed changes in slope that weren't observed in force-displacement measurements of the same stack in shake table tests (the special instrument designed to measure this response in situ under the equipment in the shake table test is discussed in section 4). This is likely because of slight misalignment between washers in the stack initially that corrects itself during the loading. To avoid this, an alternative approach was devised, where the compressive loading was applied to the stack through a loading frame and guiding rod as illustrated in Figure 6a. This arrangement is closer to how the washer stack is installed under the equipment. The guiding rod prevents any initial misalignment and subsequent realignment. The resulting force-displacement measurement, shown in Figure 6b, does not have any unexpected changes in slope. Indeed the in situ

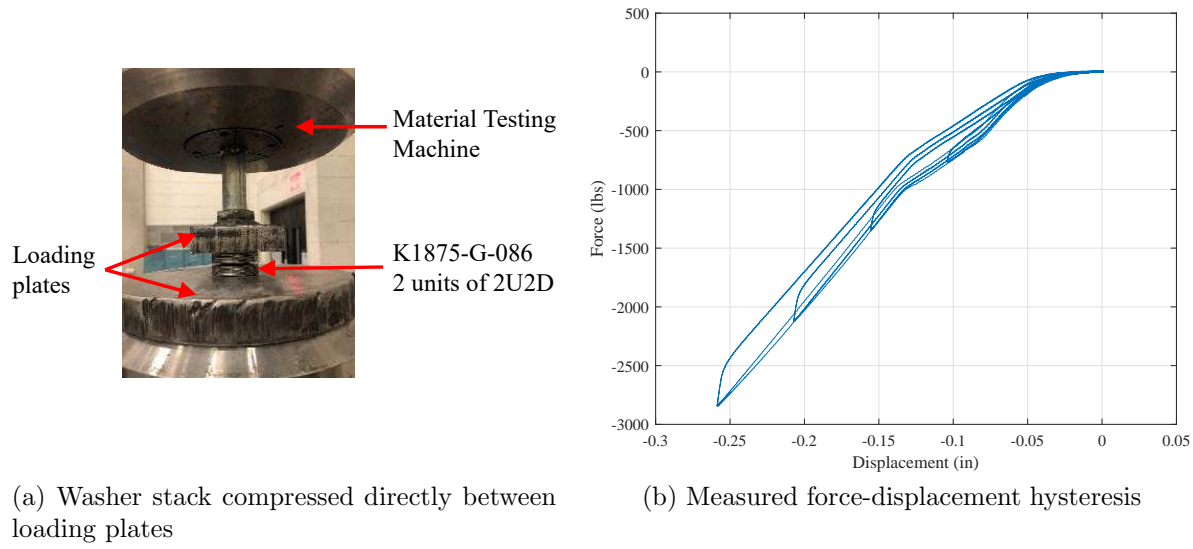


Figure 5: Washer stack force-displacement response measurement by *compressing the stack directly* in the materials testing machine; force-displacement response exhibits unexpected changes in slope.

measurements from the shake table tests follow these curves closely as seen in Figure 7. Figure 8 shows force-displacement curves for two configurations of the K1750-J-057 washers. They exhibit the reduction in stiffness with loading noted in Figure 2 due to their higher  $h/t$  ratio.

## 4 Shake table experiments

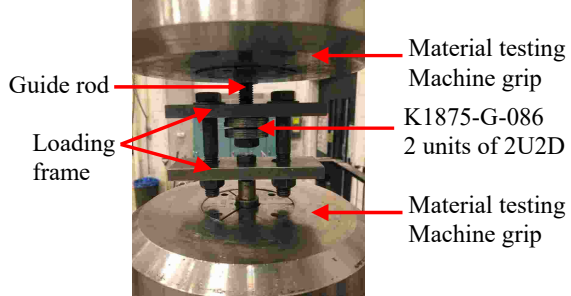
In this chapter, shake table experiments on the CVT equipped with Belleville washer stacks are described. The experimental setup, instrumentation, and washer installation process are detailed. The primary purpose of these experiments is to obtain measurements in support of the analysis procedure outlined in section 2. Consequently, special instruments were used to measure the washer response *in situ*. Instrumentation was also designed with redundancy in mind, so that the same quantity is measured by multiple means and can be cross-checked. Some other checks such as sums of forces are moments are performed to confirm the integrity of the measurements.

### 4.1 Test setup

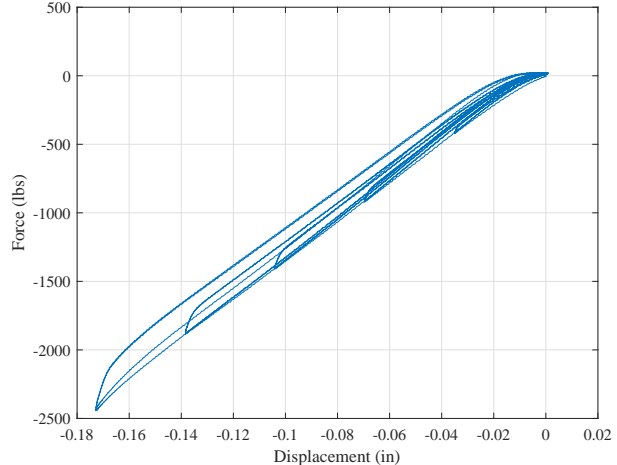
Figure 9 shows the CVT mounted on the shake table. The CVT is mounted on a pedestal referred to as the “spool”, which in turn is mounted on the shake table. The spool consists of a 10-in diameter  $\frac{1}{2}$ -in thick 16.5-in tall steel tube with a 22in  $\times$  17in steel plate welded on top (to match the base dimensions of the CVT). Figure 9 also shows the direction convention  $X$  along the East-West direction,  $Y$  along the North-South direction and  $Z$  along the vertical direction. The distance between the mounting holes at the base of the CVT is greater in the  $Y$  direction than in  $X$  direction (resulting, for example, in the  $Y$  frequency direction than in the  $X$  direction). The Belleville washer stacks are installed between the CVT base and the spool, details of which are elaborated below.

### 4.2 Instrumentation

An overview of response quantities measured and corresponding instrumentation is provided in Figure 10. Table 2 contains a detailed summary. In addition to these response quantities that are measured directly, further response quantities are derived indirectly from them. These quantities as well as the process used to derive them are summarized in Table 3. A specialized instrument in Table 2, designed in this project to

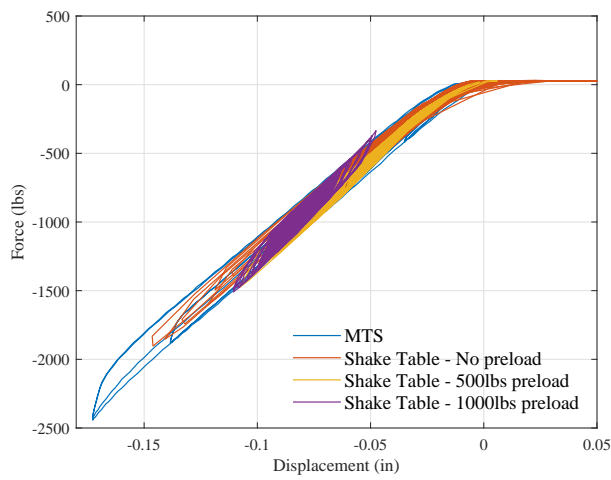


(a) Washer stack compressed through a loading frame with guiding rod

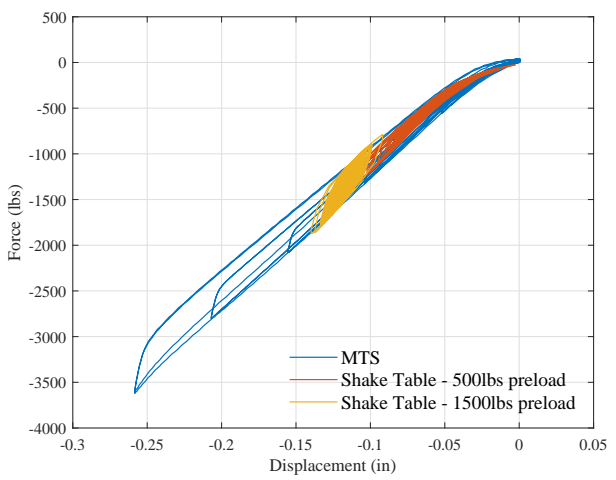


(b) Measured force-displacement hysteresis

Figure 6: Washer stack force-displacement response measurement by *compressing the stack through a loading frame with guiding rod*; this is closer to how washers are mounted under the equipment, and the force-displacement response is clean.



(a) 2 units of 2U2D K1875-G-086



(b) 3 units of 3U3D K1875-G-086

Figure 7: Measured force-displacement curves for two configurations. The legend MTS denotes measurement from the materials testing machine through the frame with guiding rod. The other curves are in situ measurements from the shake table at different preload levels. The in-situ measurements follow the testing machine results closely, confirming that the washer stack response can be characterized fully using simply a materials testing machine.

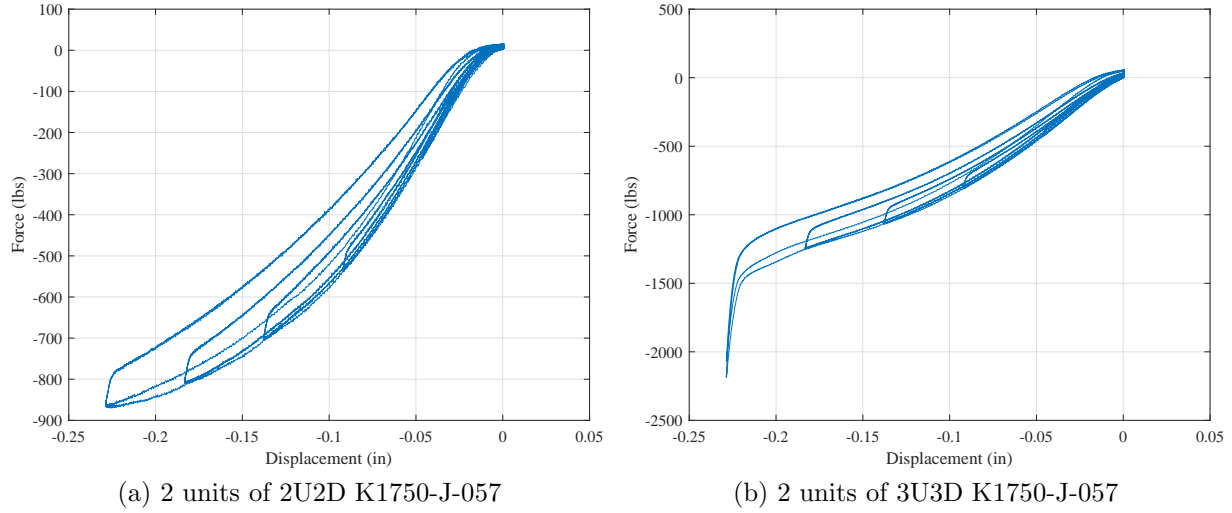


Figure 8: Measured force-displacement curves for two configurations with the K1750-J-057 washers. They have a softening behavior because of their larger  $h/t$  ratio (cf. Figure 2)

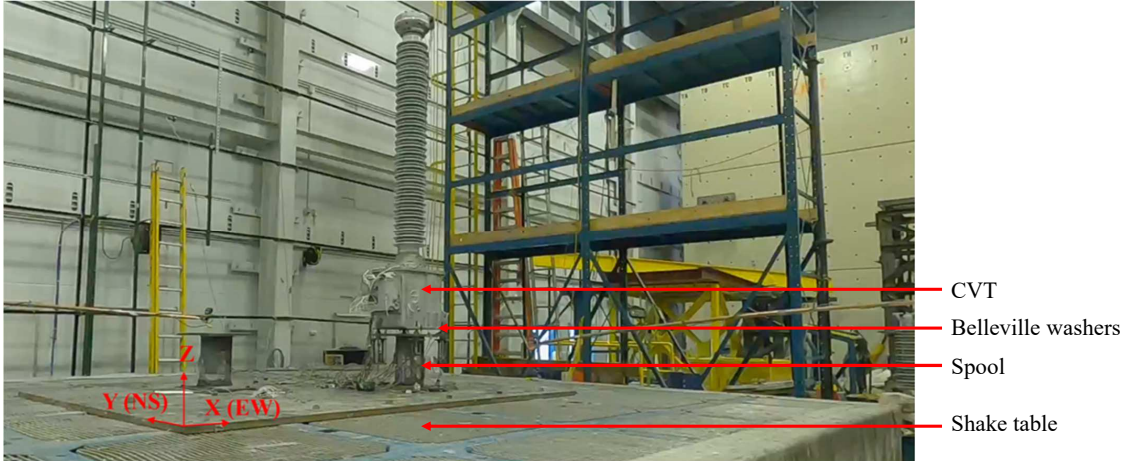


Figure 9: CVT mounted on shake table

measure the force in a washer stack in situ is the Load Washer Alternate (LWA) shown in Figure 11. It consists of a frame made of a frame consisting of two plates and two  $\frac{3}{4}$ -in threaded rods. The guiding rod of the Belleville washer stacks goes through a hole in the top plate, and connects to a load cell attached to the bottom plate. When the washer stack right above the top plate is compressed, the guiding rod develops tension that is measured by the load cell. Thus the load cell measures the compression in the Belleville washer stack below the spool plate.

### 4.3 Determination of CVT inertia properties

For further analysis, the mass, mass moment of inertia and center of mass position of the CVT must be determined. The mass is obtained simply from the measured weight. The center of mass position is determined by balancing the CVT horizontally using a crane. The mass moment of inertia is computed from the frequency measured by mounting the CVT on springs of known stiffness (Figure 12) using the method outlined in Figure 13. A summary of the inertia properties of the CVT is shown in Table 4.

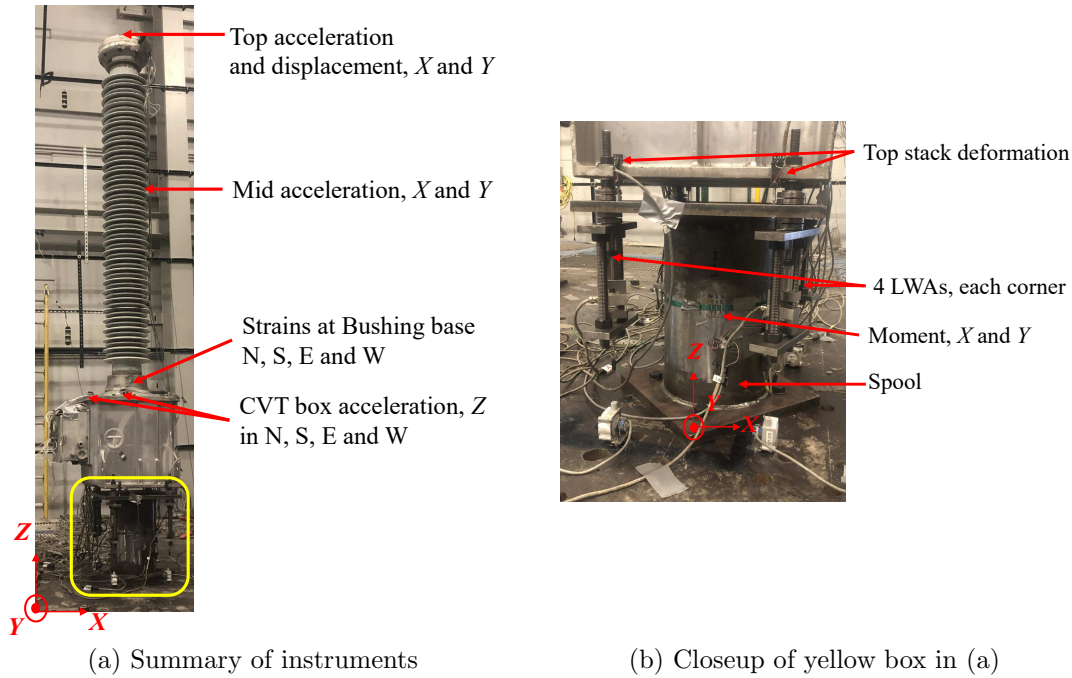


Figure 10: Instrumentation details

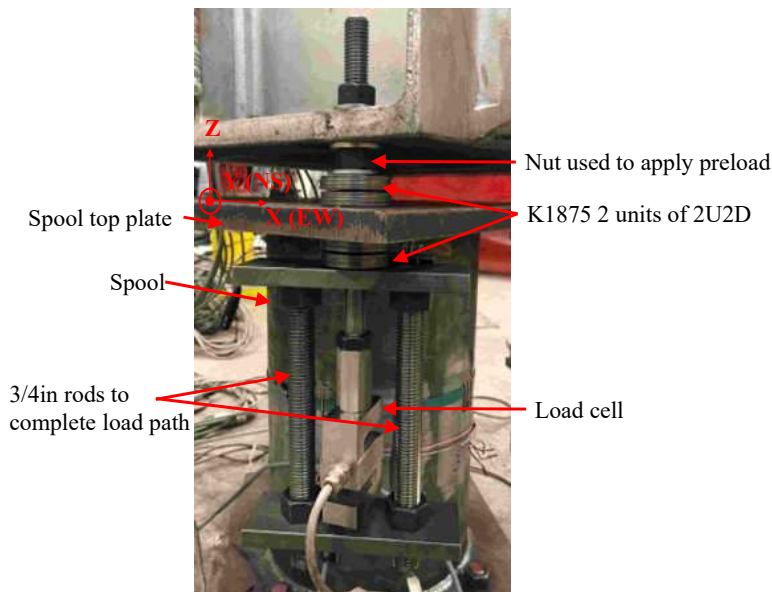


Figure 11: Details of Load Washer Alternate (LWA) and preloading process

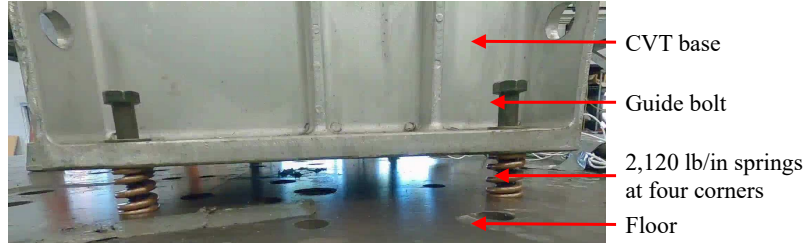


Figure 12: CVT mounted on springs to estimate mass moment of inertia indirectly from measured frequency

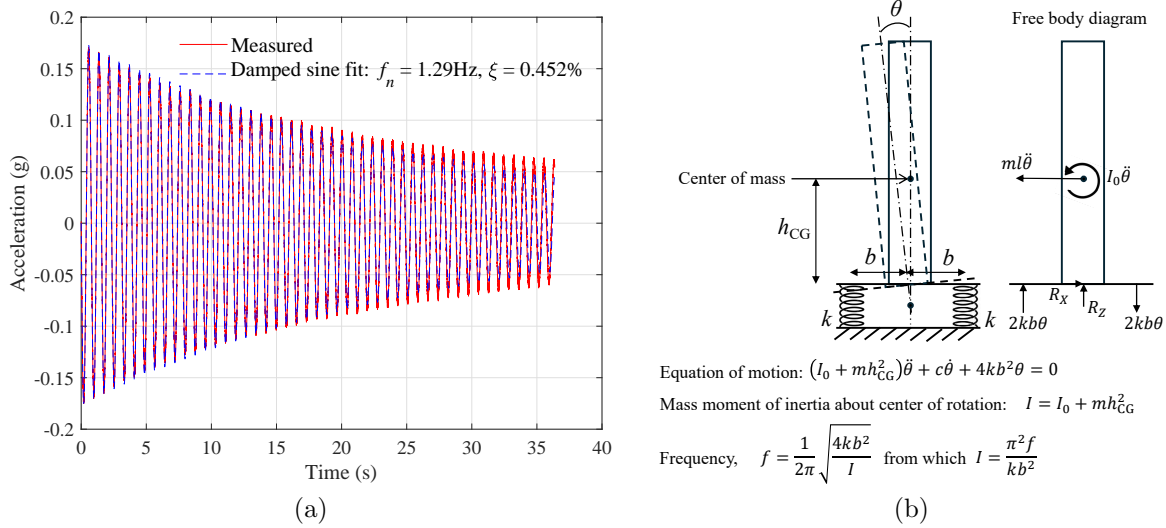


Figure 13: Acceleration measured when CVT is mounted on springs and the resulting frequency fit, and process to compute CVT mass moment of inertia from measured frequency; the dimension  $b$  is 6.375in in the  $X$  direction and 9.25in in the  $Y$  direction.

Table 2: Summary of measured response quantities and corresponding instruments

No.	Response quantity	Instrument
1	Top $X$ and $Y$ displacement components	String potentiometers attached to frames outside the shake table, so these measure absolute displacements
2	Top $X$ and $Y$ acceleration components	One 3D accelerometer
3	$X$ and $Y$ accelerations at insulator mid-height	Two 1D accelerometers
4	$Z$ accelerations at N, S, E, W locations on CVT box	Four 1D accelerometers
5	Insulator base moment	Strain gages at N, S, E, W locations at insulator base, calibrated to measure base moment
6	Displacements at 4 locations of the base of the CVT relative to the spool plate	Four linear potentiometers
7	Tension forces in rods going through the four washer stacks	Four specially designed instruments called “load washer alternates” LWAs (see below)
8	Two bending moment components in the spool ( $M_{\text{spool}}$ )	Two full-bridge strain gage circuits, one for $X$ bending moment and the other for $Y$
9	Shake table accelerations	3D accelerometers
10	Shake table displacement	String potentiometers

#### 4.4 Washer stack installation

Special care is exercised in controlling the preload when installing the Belleville washer stacks. The stacks are installed on the spool plate with out the CVT present. The stacks at each corner are preloaded independently by tightening the nut at the top (Figure 11) by a prescribed number of turns corresponding to fraction of flattening displacement targeted in the washer stacks. The force in the bottom stack is simultaneously monitored using the LWA to make sure that the load corresponds to the stack deflections in accordance with the force-deformation relationship measured in the tests described in section 3. The CVT is then seated on the four top nuts, and fixed in place using four nuts above the CVT base plate.

#### 4.5 Test configurations and protocol

Pull tests were performed in the X and Y directions with the CVT fixed directly to the spool plate to calibrate to the bending moment load cells in the spool and the strain gages at the insulator base to bending moment. The washer configurations shown in Table 5 were tested. All configurations were double acting – there were washer stacks above and below the spool plate. For each configuration, a sequence of tests consisting of low-level broad-band random input (for baseline system identification) and the CERL ground motion with increasing amplitude levels (culminating at 0.5g) were applied first in the X direction and then in the Y direction. The 5%-damped test response spectra of the applied motion are shown in Figure 14.

#### 4.6 Correlating measured forces and accelerations

Various measured forces and accelerations are correlated to gain confidence in the measurements to then compare with analysis predictions in section 5. Consider the free body diagram in Figure 15. The dimensions

Table 3: Response quantities derived indirectly from measurements

No.	Derived response quantity	Symbol*	Method of computation
i	Rigid-body translational and rotational acceleration of CVT at center of mass	$\ddot{x}_t, \ddot{\theta}$	Linear fit to acceleration components rows 2–4 in Table 2. A good fit here demonstrates the CVT can be idealized as a rigid body.
ii	Total rotation of CVT	$\theta$	Linear fit to CVT displacements (row 1) and shake table displacements (row 10) in Table 2.
iii	Rotation of CVT relative to spool plate	$\theta_w$	Linear fit to displacements in row 6 of Table 2.
iv	Restoring moment generated by washer stacks (and spool plate)	$M_{\text{CVT}}$	Twice the moment computed from the four LWAs (row 7 of Table 2, see Figure 4-3 for details).
v	Deflection of spool plate		Difference of rows ii and iii above

\*The symbols listed here are in reference to dynamics in the  $X$  (East-West) direction, corresponding quantities in the  $Y$  (North-South) direction will be labeled similarly, but not shown here

Table 4: Summary of CVT inertia properties

Parameter (Unit)	Description	Value
$m$ (lb-s <sup>2</sup> /in)	Mass	940/386.4
$h_{\text{CG}}$ (in)	Height of center of mass from CVT base	35-1/16
$I$ (lb-s <sup>2</sup> -in)	Mass moment of inertia about center of rotation	5500
$I_0$ (lb-s <sup>2</sup> -in)	Mass moment of inertia about center of mass	2500

used in this free body diagram are summarized in Table 6. The equilibrium equations

$$\begin{aligned} \sum F_X &= 0 \implies V = m\ddot{x}_t \\ \sum M &= 0 \implies M_{\text{spool}} = -I_0\ddot{\theta} - VL = -I_0\ddot{\theta} - m\ddot{x}_t L \end{aligned} \quad (2)$$

The correlation between the left and right hand sides of the second of equations (2), each of which is obtained using independent measurements, is verified in Figure 4-8, demonstrating consistency.

Next consider the free body diagrams shown in Figure 16. In this figure,  $F_{it}$  and  $F_{ib}$  stand for the force in the top and bottom washer stacks at corner  $i$ , and  $F_i$  for the force in the corresponding guide rod. Superscript “pre” denotes the preload component of these forces and  $\Delta$  denotes the change due to the CVT weight and during dynamic response. Since each assembly of washers under preload is in equilibrium,

$$F_{ib}^{\text{pre}} = F_{it}^{\text{pre}} = F_i^{\text{pre}} \quad (3)$$

Furthermore,

$$F_1^{\text{pre}} = F_2^{\text{pre}} = F_3^{\text{pre}} = F_4^{\text{pre}} \quad (4)$$

since all the assemblies are preloaded to the same level. Summing moments about the center of rotation  $O$ ,

$$\begin{aligned} M_{\text{spool}} - (F_1^{\text{pre}} + \Delta F_1 + F_4^{\text{pre}} + \Delta F_4)b + (F_2^{\text{pre}} + \Delta F_2 + F_3^{\text{pre}} + \Delta F_3)b \\ + (F_{1t}^{\text{pre}} - \Delta F_{1t} - F_{4t}^{\text{pre}} + \Delta F_{4t})b - (F_{2t}^{\text{pre}} - \Delta F_{2t} - F_{3t}^{\text{pre}} + \Delta F_{3t})b - Vr = 0 \end{aligned} \quad (5)$$

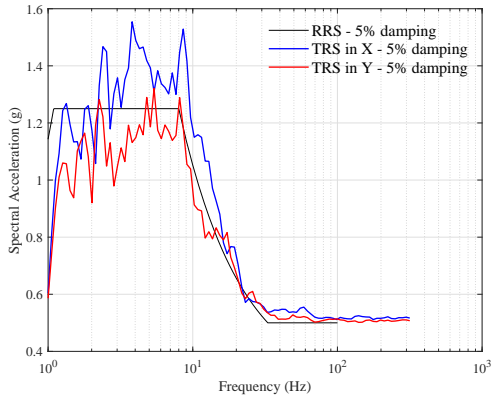


Figure 14: 5%-damped test response spectra of applied CERL motion compared with required response spectrum

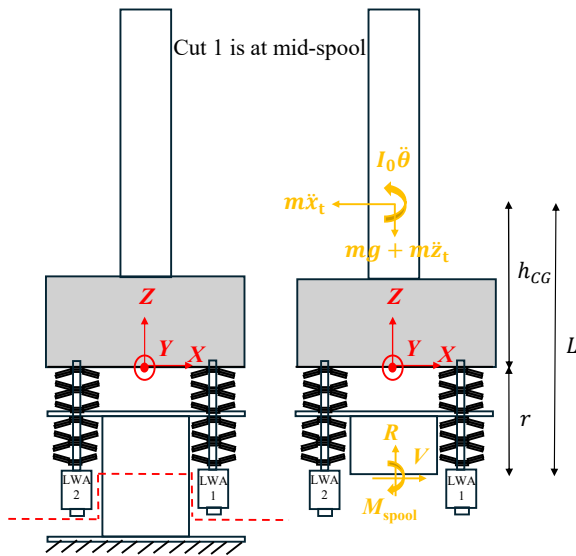


Figure 15: Free body diagram with mid-spool cut

Table 5: Summary of configurations tested

Washer	Configuration	Pre-load (% of flattening load)
K1875-G-086	2 units of 2U2D	0lb (0%)
		500lb (25%)
		1000lb (50%)
K1750-J-057	3 units of 3U3D	500lb (17%)
		1500lb (50%)

Table 6: Summary of CVT inertia properties

Dimension	Description	Value (in)
$r$	Distance between CVT base and mid spool	11
$L$	Distance between CVT center of mass and mid spool	46-1/16
$l$	Distance between CVT center of mass and center of rotation; this is obtained by fitting the equation $\ddot{x}_g + \ddot{\theta} = \ddot{x}_t$	38

Using equation (3) to cancel out the  $F_i^{\text{pre}}$  and  $F_{it}^{\text{pre}}$ , and substituting for  $V$  from equation (2),

$$M_{\text{spool}} - (\Delta F_1 + \Delta F_4)b + (\Delta F_2 + \Delta F_3)b - (\Delta F_{1t} + \Delta F_{4t})b - (\Delta F_{2t} + \Delta F_{3t})b - m\ddot{x}_t r = 0 \quad (6)$$

A further assumption is made that

$$\Delta F_i = \Delta F_{ib} = \Delta F_{it} \quad (7)$$

This does not follow from equilibrium, but is taken to be true based on symmetry/compatibility of top and bottom stack deformations. Then equation (6) becomes

$$M_{\text{spool}} = 2(\Delta F_1 + \Delta F_4 - \Delta F_2 - \Delta F_3)b + m\ddot{x}_t r \quad (8)$$

Using equation (4), this can be further written as

$$M_{\text{spool}} = \underbrace{2(F_1 - F_2 - F_3 + F_4)b}_{M_{\text{CVT}}} + m\ddot{x}_t r \quad (9)$$

where  $F_i = F_i^{\text{pre}} + \Delta F_i$  is the directly the force measured by LWA  $i$ . Verifying this relationship, which again involves multiple independent measurements, adds further confidence in the measured data for comparison with analysis. In particular, this confirms the thinking that the in-situ behavior of the washer stacks can be determined from the materials testing machine measurements. This comparison is shown in Figure 17. A final free body diagram, Figure 17, is considered in relation to the insulator base moment. The mass and mass moment of inertia of the insulator alone are not known, however its center of mass is assumed to be at mid-height. Summing the moments about the insulator base,

$$M_{\text{ins}} = -I_{0\text{ins}}\ddot{\theta} - m_{\text{ins}}\ddot{x}_{t,\text{ins}}L_1 \quad (10)$$

Substituting the kinematics,  $\ddot{x}_{t,\text{ins}} = \ddot{x}_g + L_2\ddot{\theta}$ ,

$$M_{\text{ins}} = -\underbrace{(I_{0\text{ins}} + m_{\text{ins}}L_1L_2)}_{I_{\text{ins}}}\ddot{\theta} - m_{\text{ins}}L_1\ddot{x}_g \quad (11)$$

The insulator mass,  $m_{\text{ins}}$ , and the net mass moment of inertia,  $I_{\text{ins}}$  are known. Equation (11) is used to fit them to measure data. The fit values are  $m_{\text{ins}} = 360/386.4\text{lb}\cdot\text{s}^2/\text{in}$  (about 40% of the total mass of the CVT) and  $I_{\text{ins}} = 3,500\text{lb-in}\cdot\text{s}^2$ . These values are used when comparing analysis results to measured insulator base moment. The measured insulator base moments are shown in Figure 4-12 and Figure 4-13.

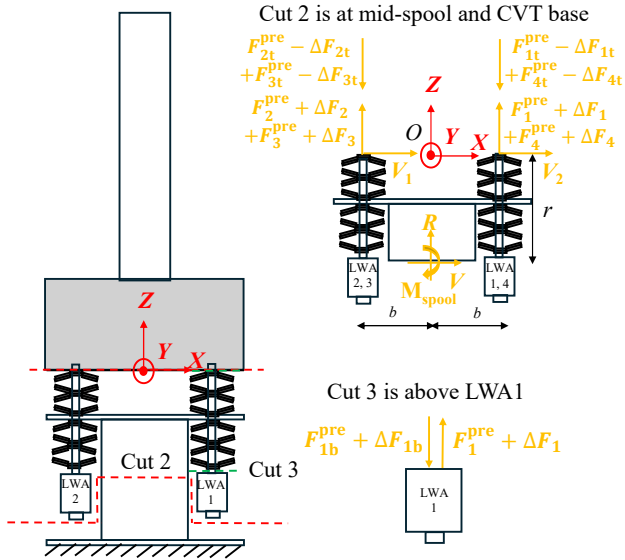


Figure 16: Free body diagrams relating moment measured at the spool with moment estimated using LWAs

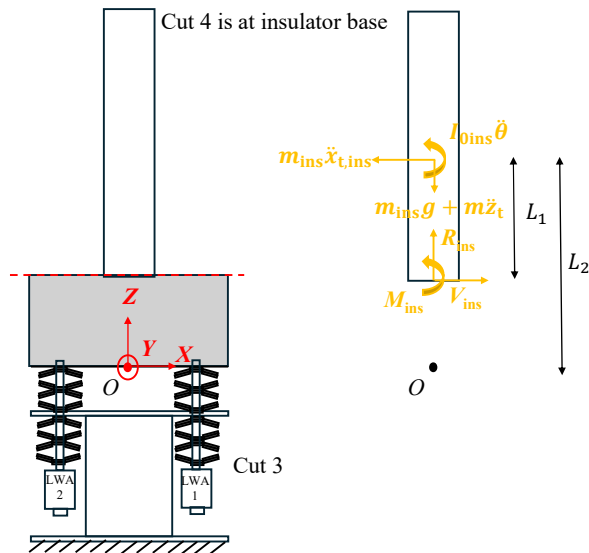


Figure 17: Free body diagram used to relate insulator base moment to measured accelerations; \$L\_1\$ is the mid-height of the insulator, \$L\_1 = in\$; \$L\_2\$ is the distance from the center of rotation to the center of mass of the insulator, \$L\_2 = in\$.

## 5 Nonlinear modeling and analysis

In this section, a nonlinear model is developed for the CVT installed on Belleville washer stacks. The CVT is modeled as a rigid body, and a hysteretic model is used to represent the moment-rotation behavior resulting from the aggregate action of the washer stacks (the type of moment-rotation hysteretic behavior seen in the measurements of Figure 4-11).

### 5.1 From stack force-displacement to system moment-rotation

The moment-rotation hysteresis behavior can be obtained from the washer stack force-displacement response, whose measure was discussed in section 3, using the process depicted in Figure 5-1. An example of this process is illustrated in Figure 5-2. The specific example shown in Figure 5-2 corresponds to a low preload (25% of flattening). In this condition, when the washer stacks on one side reach the highest deformation (bottom left of Figure 5-2), the stacks on the other side relax entirely, losing preload (bottom right of Figure 5-2). The net effect is a softening of the moment-rotation behavior near the extremes (top right of Figure 5-2).

### 5.2 Modeling moment-rotation hysteresis

The moment-rotation behavior decomposed into two parallel components – one elastic and one hysteretic as illustrated in Figure 18. The split is given by

$$M_{\text{CVT}} = K\theta_w + M_{\text{HYS}} \quad (12)$$

for cases with sufficient preload as in Figure 5-3(a) and by

$$M_{\text{CVT}} = K\tanh(\alpha\theta_w) + M_{\text{HYS}} \quad (13)$$

for cases with insufficient preload as in Figure 5-3(b), the tanh function capturing the S shape. The hysteretic component is represented using what is commonly referred to as the Bouc-Wen model [23, 24] (for a description of this model using notation similar to that used here, see [25, 26], and is given by

$$\dot{M}_{\text{HYS}} = k \left( 1 - \left| \frac{M_{\text{HYS}}}{M_{\text{yield}}} \right|^N (\eta + (1 - \eta)\text{sgn}(M_{\text{HYS}}\dot{\theta}_w)) \right) \dot{\theta}_w \quad (14)$$

where  $M_{\text{yield}}$  is the yield moment, and  $N$  and  $\eta$  are parameters that control the shape of the hysteresis. For an explanation of these parameters, see [27]. Figure 19 shows a comparison of the model with the measured moment-rotation behavior when the model is driven by the measured rotation of the CVT relative to the spool plate ( $\theta_w$ ). In constructing the full system model, the flexibility of the spool plate must be incorporated as well; this is recognized when comparing the magnitudes of the plate deformation (see Table 3), washer deformation and total rotation of the CVT in Figure 5-5.

### 5.3 Summary of nonlinear dynamic model

Combining the moment-rotation model of equations (12) and (13) or (14) with the equation of motion of the CVT (considered as a rigid body), and including the flexibility of the spool plate results in the full nonlinear model of the Belleville washer-protected CVT:

$$\begin{aligned} &\text{Equation of motion of CVT: } (I_0 + ml^2)\ddot{\theta} + M_{\text{CVT}} = 0ml\ddot{x}_g \\ &\text{Hysteretic model (equation (14) rewritten): } \dot{M}_{\text{HYS}} = k(1 - H_1 H_2)\dot{\theta}_w \end{aligned} \quad (15)$$

where  $H_1 = \left| \frac{M_{\text{HYS}}}{M_{\text{yield}}} \right|^N$ ,  $H_2 = (\eta + (1 - \eta)\text{sgn}(M_{\text{HYS}}\dot{\theta}_w))$ ,  $M_{\text{CVT}}$  given either by equation (12) or (13), the spool plate deformation,  $\theta_p = \frac{M_{\text{CVT}}}{K_p}$  ( $K_p$  p being the spool plate stiffness),  $\theta_w = \theta - \theta_p$  and  $\dot{\theta}_w = \left( \frac{K_p}{K_p + k(1 - H_1 H_2) + K} \right) \dot{\theta}$  for sufficient preload and  $\dot{\theta}_w = \left( \frac{K_p}{K_p + k(1 - H_1 H_2) + K\alpha(1 - \tanh^2(\alpha\theta_w))} \right) \dot{\theta}$  for insufficient preload. Solutions to the differential equations (15) together with these auxiliary equations are computed using the solver `ode15s` in MATLAB [28]. The insulator moment can be calculated as an output of the analysis using equation (11).

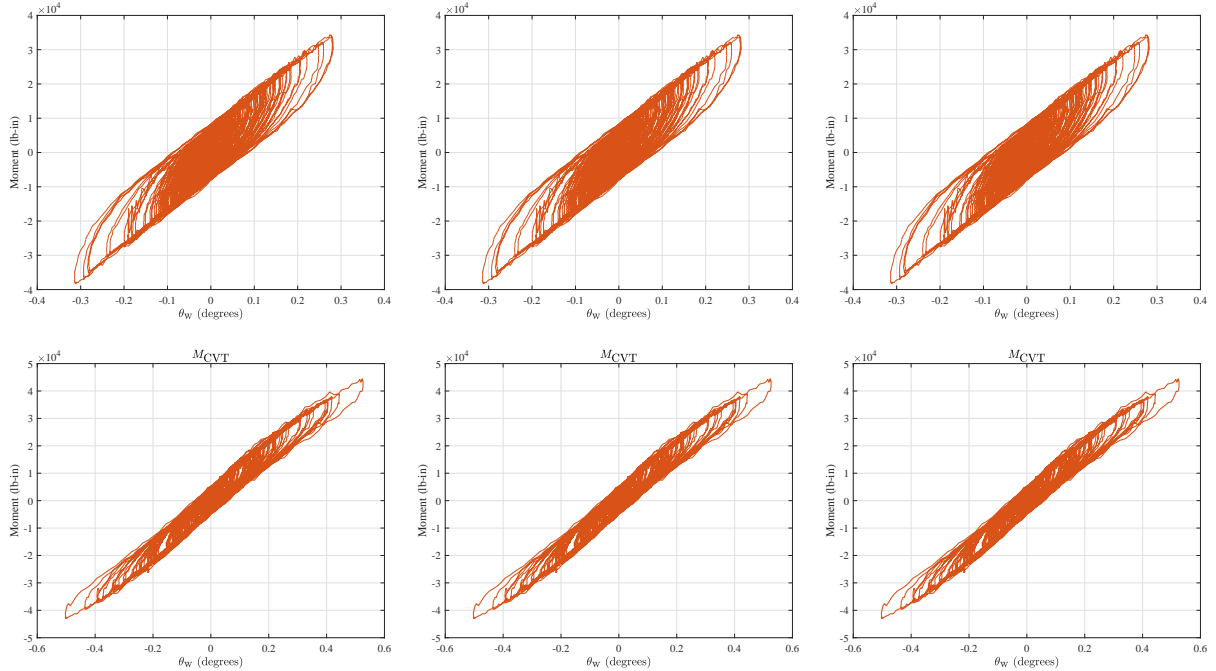


Figure 18: Parallel decomposition of moment-rotation behavior into elastic and hysteretic components (example shown for 2 units of 2U2D).

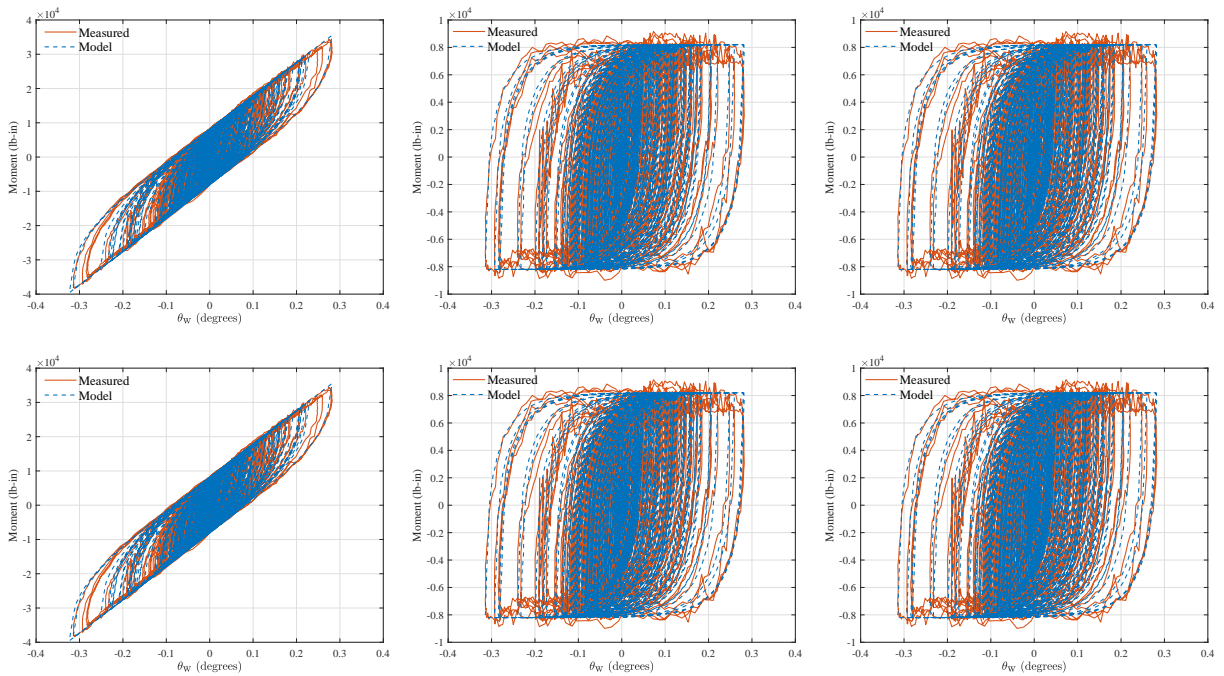


Figure 19: Comparison on model and measured moment-rotation behavior when the model is driven by the measured  $\theta_w$  as input (example shown for 2 units of 2U2D).

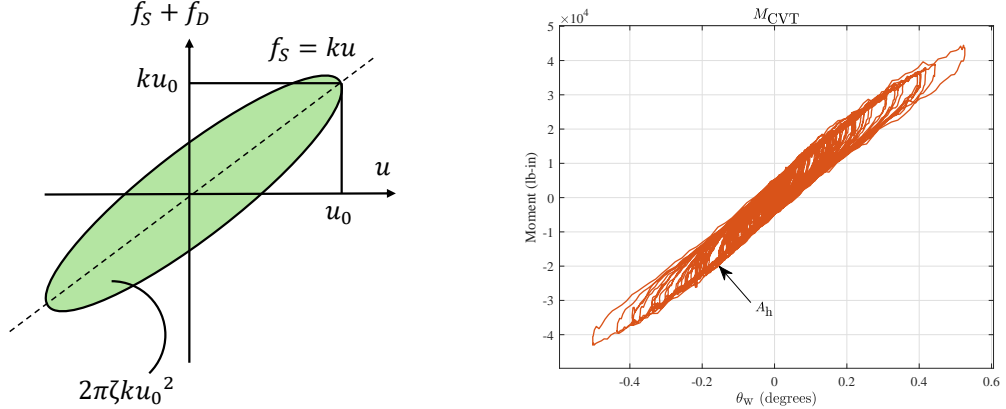


Figure 20: Concept of graphically obtaining equivalent stiffness and damping ratio.

## 5.4 Analysis results

As examples, analysis results are shown for 2 cases, but with the 2 units of 2U2D configuration under 0.5g CERL motion in the X direction, one case with 50% preload and another with 25% preload in Figure 5-6 and Figure 5-7.

## 6 Equivalent linear modeling

In the previous section, the Belleville washer-protected CVT system was analyzed using a nonlinear dynamic procedure. In this section, an alternate approach is presented using an equivalent linear approach. This approach may be better suited for practical use as well as provides insights in terms of system frequency and damping ratio. First, an equivalent linear model obtained by fitting to experimental measurements is presented; the frequencies and damping ratios so obtained are used as reference for the second approach. In the second approach, equivalent stiffnesses and damping ratios are obtained graphically from the moment-rotation hysteresis curves.

### 6.1 Equivalent frequency and damping ratio from measurements

An equivalent linear model can be obtained from experimental measurements by fitting a linear model to it. Here, this is done using the subspace linear system identification method [29]. Figure 6-2 shows a comparison of such a linear fit with measured responses. Table 7 summarizes equivalent frequencies and damping ratios for all the configurations tested. Approximate equivalent stiffness, frequency and damping ratio can be obtained graphically as illustrated in Figure 20. The equivalent stiffness,  $k_{\text{eq}}$ , is obtained as the ratio of the difference between the positive and negative peak moments and the different between the peak positive and negative rotations. The frequency is then

$$f = \frac{1}{2\pi} \sqrt{\frac{k_{\text{eq}}}{I_0 + mh_{\text{CG}}^2}} \quad (16)$$

and the damping ratio is obtained by equating the area of the hysteresis,  $A_h$ , to that of a viscous damper undergoing the same peak displacement at steady state with frequency  $f$  [30]

$$\xi = \frac{A_h}{2\pi k_{\text{eq}} u_0^2} \quad (17)$$

where these formulae parallel equations (17.2-4) and (17.2-5) of Chapter 17 of ASCE 7-16 on Seismically Isolated Structures [31].

Table 7: Summary of findings from experimental measurements and equivalent linear modeling for 0.5g CERL excitation. Damping ratios in parentheses denote those obtained by the procedure in 6.1.

Configuration	CVT fixed on spool (reference)		K1875-G-086 2 units of 2U2D				K1875-G-086 3 units of 3U3D			
			0%	25% (500lbs)	50% (1000lbs)	17% (500lbs)	50% (1500lbs)			
Preload level	-		0%	25% (500lbs)	50% (1000lbs)	17% (500lbs)	50% (1500lbs)			
Direction of excitation	X	Y	X	Y	X	Y	X	Y	X	Y
Natural frequency (Hz)	6.9	9.4	2.9 (3.0)	4.0 (4.3)	3.6 (3.5)	5.1 (5.1)	4.1 (3.8)	5.5 (5.4)	3.6 (3.6)	5.1 (5.0)
Damping ratio (%)	0.5	0.6	3.9 (3.6)	3.7 (3.4)	6.5 (7.1)	6.4 (8.7)	9.9 (14.2)	8.1 (13.6)	7.8 (8.2)	7.3 (9.9)
Maximum insulator base moment ( $\times 10^4$ lb-in)	5.1	4.5	3.5	4.0	2.9	3.2	2.4	3.3	2.7	3.0
Maximum relative terminal displacement (in)	0.9	0.6	3.4	2.1	1.8	1.1	1.4	1.0	1.8	1.1
									1.2	0.9

## 6.2 Response spectrum interpretation

It can be seen from Table 6-1 that the insulator base moment is reduced in all configurations relative to the fixed base case, and by over 50% in the  $X$  direction and by over 25% in the  $Y$  direction for the cases with sufficient preload. This however comes at the expense of greater terminal displacement, about 50% greater for the cases with highest preload. These effects are similar to that of seismic isolation. These effects can be better understood by mapping the frequencies and damping ratios of the different configurations on a spectral plot as seen in Figure 21. For each configuration, the abscissa is the frequency and the ordinate is the spectral acceleration obtained from the equations in [32] for the damping ratio of that configuration. The picture conveys the relative effectiveness of the different Belleville washer configurations with respect to the reference configuration. There is a frequency reduction that for the configurations tested does not play a major role in reducing base moments. The biggest effect is the increased damping. While such deductions can be made from the figure, the main takeaway is that with the tools developed in this project, a similar evaluation can be done for any other arrangement of washers by modeling and analysis. For example, a different configuration may be designed that further reduces frequency while increasing damping, trading off lower insulator base moment with increased terminal displacement.

## 7 Summary and concluding remarks

### 7.1 Executive summary

A modeling procedure has been developed to predict the seismic response of rigid equipment such as CVTs equipped with Belleville washer stacks at the base for seismic protection. The procedure allows for nonlinear dynamic analysis or an equivalent linear analysis, and is outlined in section 2. The starting points are (a) the force-displacement hysteretic behavior of an individual stack that can be readily obtained by cyclic loading in a materials test machine, (b) inertia properties of the CVT – mass, mass moment of inertial and center

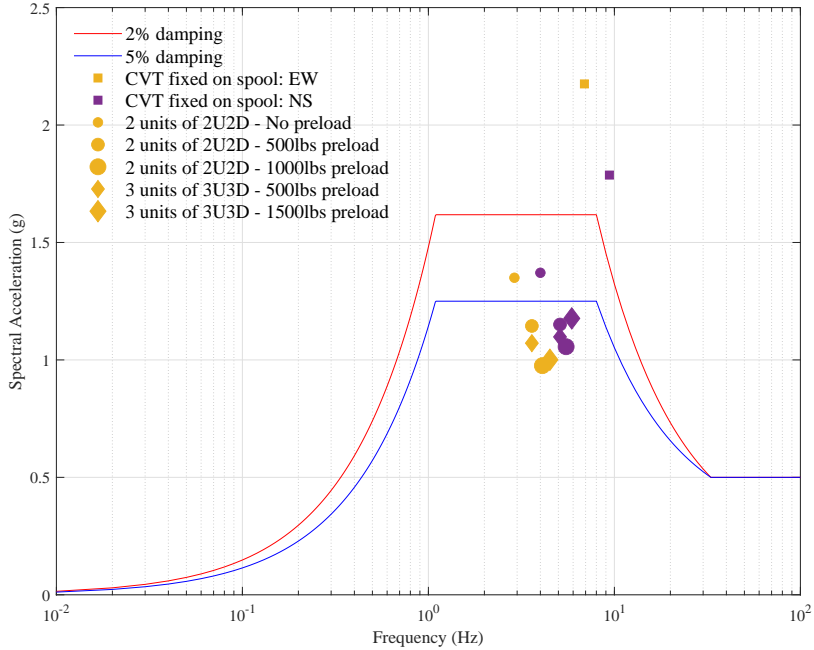


Figure 21: Frequencies and damping ratios corresponding to different Belleville washer configurations overplotted on the 2%- and 5%-damped required response spectrum (RRS) from IEEE 693-2018 [32].

of mass location. With this, the seismic response can be predicted reliably. This has been validated with experiments on an earthquake simulator (shake table). Special instrumentation was developed to obtain detailed in situ measurements of the behavior of the washer stacks in the shake table experiments. Validation using these measurements provides confidence that the analysis procedure can be used to inform decisions when installing Belleville washer devices in the field. The process also parallels procedures in ASCE 7-16 for seismic isolators. The washer stacks essentially act as seismic isolators, reducing the frequency and increasing the damping. They are effective in reducing the insulator base moment. As is the case with seismic isolation systems, reduction is base moment has to be traded off with increase in terminal displacement.

## 7.2 Outstanding research questions

Some outstanding research questions remain:

Testing and modeling with different washer types; only one washer type has been studied completely (K1875-G-086). A second washer type has been studied partially (K1750-J-057), but some issues were discovered and are being remedied. It will be useful to complete the study with the K1750 washer type, as well as one other washer type from a different vendor.

Testing and modeling beyond flattening load: When subject to earthquake larger than what the spring washer protective system is designed for, the washer is likely to flatten, causing a different type of dynamics. It will be useful to study this performance under extreme loading. This is similar to when a base isolation system hits its displacement limit, which is considered in the design.

Testing and modeling single acting configuration: Thus far, we have only test cases with the spring washers in a single acting configuration, but that one configuration revealed promising behavior consisting of flag-shaped hysteretic behavior. It will be useful to study this further.

## References

- [1] R. Couch and R. Deacon, "Procedures and criteria for increasing the earthquake resistance level of electrical substations and special installations," tech. rep., Agbabian Associates, El Segundo, CA (USA), 1973.
- [2] R. S. Cochran, "Seismic base isolation of a high voltage transformer," in *Electrical Transmission and Substation Structures 2015*, pp. 413–425, 2015.
- [3] L. Kempner Jr. and M. Riley, "High voltage transformer base isolation," in *Proceedings of the 11th Canadian Conference on Earthquake Engineering*, 2015.
- [4] K. Oikonomou, M. C. Constantinou, A. M. Reinhorn, and L. Kempner Jr, "Seismic isolation of high voltage electrical power transformers," *MCEER Technical Report MCEER-16*, vol. 6, 2016.
- [5] M. A. Saadeghvaziri, B. Feizi, L. Kempner Jr, and D. Alston, "On seismic response of substation equipment and application of base isolation to transformers," *IEEE Transactions on power delivery*, vol. 25, no. 1, pp. 177–186, 2009.
- [6] N. Blunt, "The Difference Between Disc Springs and Belleville Washers." [https://www.spirol.com/assets/files/disc\\_wp\\_differences\\_between\\_disc\\_springs\\_and\\_belleville\\_washers\\_us.pdf](https://www.spirol.com/assets/files/disc_wp_differences_between_disc_springs_and_belleville_washers_us.pdf). Accessed: 11-8-2025.
- [7] J. E. Shigley and C. R. Mischke, *Standard handbook of machine design*. New York, NY: McGraw-Hill, 2004.
- [8] G. Ashworth, "The disk spring or belleville washer," *Proceedings of the Institution of Mechanical Engineers*, vol. 155, no. 1, pp. 93–100, 1946.
- [9] J. O. Almen and A. Laszlo, "The uniform-section disk spring," *Journal of Fluids Engineering*, vol. 58, no. 4, pp. 305–314, 1936.
- [10] Y. Zhou, D. Wang, Z. Qiu, Z. Wei, W. Chen, and R. Zhu, "Modeling of disc springs based on energy method considering asymmetric frictional boundary," *Thin-Walled Structures*, vol. 190, p. 110971, 2023.
- [11] M. Korytov, V. Shcherbakov, V. Titenko, I. Kashapova, and V. Derkach, "Use of the belleville spring package in the vibration protection mechanism of the operator's seat," in *Journal of Physics: Conference Series*, vol. 2182, p. 012056, IOP Publishing, 2022.
- [12] C. Maletta, L. Filice, and F. Furgiuele, "Niti belleville washers: Design, manufacturing and testing," *Journal of intelligent material systems and structures*, vol. 24, no. 6, pp. 695–703, 2013.
- [13] Solon Manufacturing Co., "Belleville Spring Washer Applications & Solutions." <https://www.solonmfg.com/washer-applications>. Accessed: 11-8-2025.
- [14] T. Fujita, "Fundamental study of three-dimensional seismic isolation system for nuclear power plants," in *Proceedings of Eleventh World Conference on Earthquake Engineering, 1996-6*, vol. 5, 1996.
- [15] S. Kitamura, T. Nakatogawa, A. Miyamoto, and T. Somaki, "Experimental study on coned disk springs for vertical seismic isolation system," *Transaction of the 17th SMiRT, Prague, Czech Republic, August, Division K, Paper# K10*, vol. 2, 2003.
- [16] S. Kitamura, S. Okamura, and K. Takahashi, "Experimental study on vertical component seismic isolation system with coned disk spring," in *ASME Pressure Vessels and Piping Conference*, vol. 41936, pp. 175–182, 2005.
- [17] S. Ramhormozian, G. C. Clifton, G. A. MacRae, and G. P. Davet, "Stiffness-based approach for belleville springs use in friction sliding structural connections," *Journal of Constructional Steel Research*, vol. 138, pp. 340–356, 2017.

- [18] M. Speicher, D. E. Hodgson, R. DesRoches, and R. T. Leon, “Shape memory alloy tension/compression device for seismic retrofit of buildings,” *Journal of materials engineering and performance*, vol. 18, no. 5, pp. 746–753, 2009.
- [19] K. E. Hill, *The utility of ring springs in seismic isolation systems*. Phd thesis, University of Canterbury, Department of Mechanical Engineering, Christchurch, New Zealand, 1995.
- [20] K. Ma, Y. Zhou, and D. Lu, “Theoretical and experimental investigation on disc spring isolation system with loading rings,” *Soil Dynamics and Earthquake Engineering*, vol. 165, p. 107655, 2023.
- [21] IEEE recommended practice for seismic design for substations, *IEEE Std 693-1984*, 1984.
- [22] Key Bellevilles Inc., “Belleville spring washer applications & solutions.” <https://keybellevilles.com/bellevilles/sampleCatalog>. Accessed: 11-8-2025.
- [23] R. Bouc, “Forced vibrations of mechanical systems with hysteresis,” in *Proc. of the Fourth Conference on Nonlinear Oscillations, Prague, 1967*, 1967.
- [24] Y.-K. Wen, “Method for random vibration of hysteretic systems,” *Journal of the engineering mechanics division*, vol. 102, no. 2, pp. 249–263, 1976.
- [25] M. V. Sivaselvan and A. M. Reinhorn, “Hysteretic models for deteriorating inelastic structures,” *Journal of engineering mechanics*, vol. 126, no. 6, pp. 633–640, 2000.
- [26] M. V. Sivaselvan and A. M. Reinhorn, “Nonlinear structural analysis towards collapse simulation: A dynamical systems approach,” 2004.
- [27] M. C. Constantinou and M. Adnane, *Dynamics of soil-base-isolated-structure systems: evaluation of two models for yielding systems. report 4*. Department of Civil Engineering, Drexel University, 1987.
- [28] The MathWorks Inc., *MATLAB version: 9.16.0 (R2024b)*. Natick, Massachusetts, 2024.
- [29] P. Van Overschee and B. De Moor, *Subspace identification for linear systems: Theory—Implementation—Applications*. Springer Science & Business Media, 2012.
- [30] A. Chopra, *Dynamic of Structures, Theory and Applications to Earthquake Engineering*. Pearson, 2023.
- [31] M. D. Loads, “Minimum design loads and associated criteria for buildings and other structures,” *Minimum Design Loads and Associated Criteria for Buildings and Other Structures*, 2017.
- [32] IEEE recommended practice for seismic design for substations, *IEEE Std 693-2018 (Revision of IEEE Std 693-2005)*, 2019.